arXiv:1402.6009v1 [cond-mat.mes-hall] 24 Feb 2014

Valley dynamics probed through charged and neutral exciton emission in monolayer WSe_2

G. Wang, L. Bouet, D. Lagarde, M. Vidal, A. Balocchi, T. Amand, X. Marie, and B. Urbaszek*

Université de Toulouse, INSA-CNRS-UPS, LPCNO, 135 Av. de Rangueil, 31077 Toulouse, France

Abstract

Optical interband transitions in monolayer transition metal dichalcogenides such as WSe_2 and MoS_2 are governed by chiral selection rules. This allows efficient optical initialization of an electron in a specific K-valley in momentum space. Here we probe the valley dynamics in monolayer WSe_2 by monitoring the emission and polarization dynamics of the well separated neutral excitons (bound electron hole pairs) and charged excitons (trions) in photoluminescence. The neutral exciton photoluminescence intensity decay time is about 4ps, whereas the trion emission occurs over several tens of ps. The trion polarization dynamics shows a partial, fast initial decay within tens of ps before reaching a stable polarization of $\approx 20\%$, for which a typical valley polarization decay time larger than 1ns can be inferred. This is a clear signature of stable, optically initialized valley polarization.

Keywords: WSe2, valley dynamics, time resolved photoluminescence, transition metal dichalcogenides, two dimensional materials

*urbaszek@insa-toulouse.fr

In strong analogy to graphene, the physical properties of transition metal dichalcogenides (TMDCs) change drastically when thinning the bulk material down to one monolayer (ML) [1]. The closely related ML materials WSe_2, MoS_2, $MoSe_2$ and WS_2 [2] have a direct bandgap in the visible region [3–5] and show strong optical absorption. ML WSe_2 is an exciting, atomically flat, two-dimensional material for electronics [6, 7], non-linear optics [8] and optoelectronics [9, 10], just as ML MoS_2 [10–12]. Current micro-and nano-electronics is based on the manipulation of the electron charge and spin. ML TMDCs provide unique and convenient access to controlling in addition the electron valley degree of freedom in k-space in the emerging field of 'valleytronics' [13–15]. The circular polarization (σ^+ or σ^-) of the absorbed or emitted photon can be directly associated with selective carrier excitation in one of the two non-equivalent K valleys (K_+ or K_-, respectively) [2, 13, 17, 18], see figure 1a. The valley polarization is protected by the strong spin-orbit splitting in the valence and conduction band [13, 16, 19], leading in principle to a high stability for the valley degree of freedom. The high circular photoluminescence (PL) polarization degree reported in time integrated measurements in ML MoS_2 [17, 20–24] and ML WSe_2 [20] seems to confirm this prediction.

The stability of the created valley polarization is crucial for manipulating the electron valley degree of freedom in transport measurements or with successive laser pulses in optical control schemes, where excitonic effects are important [25, 26]. Recent time resolved studies show PL emission times in the picosecond range [27, 28] and pump-probe measurements in ML MoS_2 have shown polarization decay times in the ps range [29, 30] corresponding to fast relaxation of the valley index. In these experiments on ML MoS_2 the neutral exciton (X^0) and the charged exciton (trion) emission cannot be clearly spectrally separated due to the broad transitions, although the evolution of the valley polarization is expected to be distinctly different for the two complexes. The neutral excitons in different K-valleys are coupled by Coulomb exchange [31], which can lead to inter-valley scattering [32, 33]. The trion polarization is expected to be far more stable as inter-valley scattering demands in this case spin-flips of individual carriers, which are energetically and spin-forbidden. This would make the trion an excellent candidate for optically initialized valley Hall experiments [33]. However, the trion valley dynamics in ML TMDCs is so far unexplored.

In time resolved PL (TRPL) experiments we uncover marked differences between the X^0 and the trion valley dynamics in ML WSe_2 as the spectrally well-separated transition can

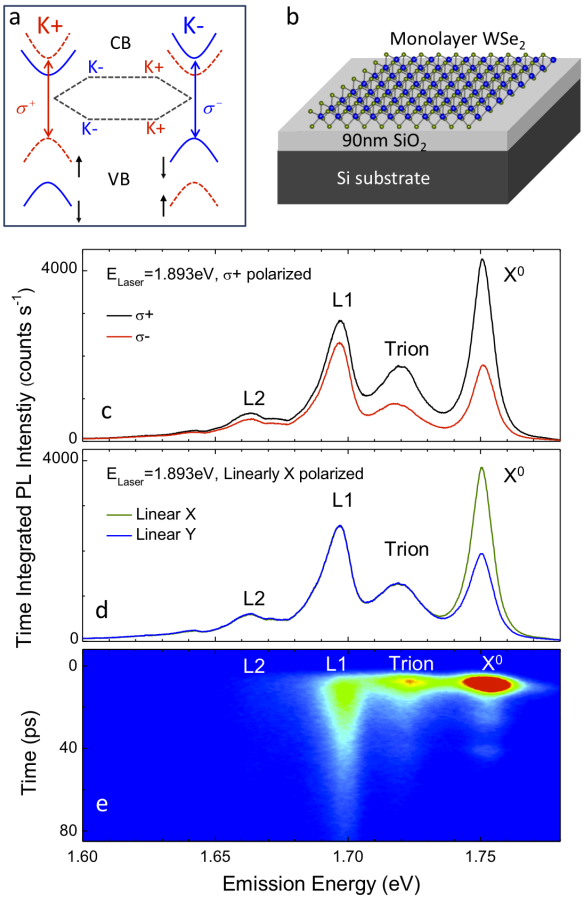

FIG. 1: (a) optical interband selection rules for monolayer WSe_2 according to [16] (b) investigated sample structure (c) Laser polarization σ^+ and E_{Laser} = 1.893 eV. PL Emission of ML WSe_2 at T=4K, the X^0, trion and localized states are marked. black (red) $\sigma^+(\sigma-)$ polarized (d) Linear Laser polarization X. green (blue) corresponds to linear X (linear Y) polarized emission. (e) Streak camera image of TRPL total intensity showing different emission times for X^0, trion and localized states. Blue (red) corresponds to zero (10000) counts.

be analysed independently at low temperature, see figure 1e. We measure a trion emission time of $\approx$ 18 ps. Following optical initialization with a circularly polarized laser, the trion PL emission reaches a stable polarization within about 12ps. For the strong, remaining polarization we can infer a decay time longer than 1ns. This is a direct experimental signature of the temporal stability of optically generated valley polarization. In contrast, the neutral exciton emission and polarization decays within a few ps. We also clearly identify localized excitons via their characteristically long emission times due to the lower dipole oscillator strength.

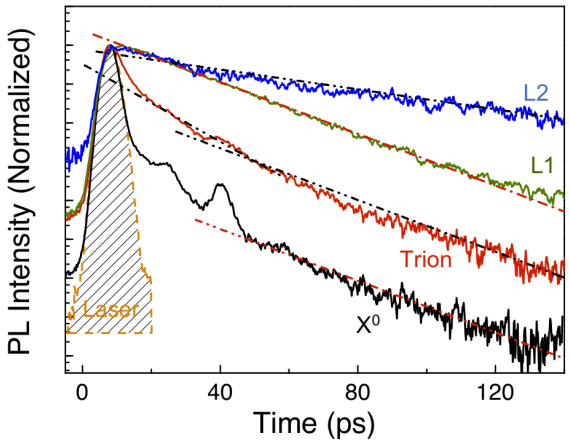

FIG. 2: **Time resolved photoluminescence.** T=4K. Normalized PL dynamics (total peak intensity) in log-scale for X^0, trion, L1 and L2. The lines show fits with exponential decays with typical times of 30 ps (X^0 and L1) and 78 ps (L2). Trion fitted with bi-exponential decay, with 18 ps and 30 ps characteristic decay times. The small peaks superimposed on the X^0 and trion dynamics come from laser reflections.

Samples and Experimental Set-up.— Monolayer WSe_2 flakes are obtained by micro-mechanical cleavage of a bulk WSe_2 crystal [34] (from 2D Semiconductors, USA) on 90 nm SiO_2 on a Si substrate, see figure 1b. The 1ML region is identified by optical contrast and very clearly in PL spectroscopy. Experiments between T=4 and 300K are carried out in a confocal microscope optimized for polarized PL experiments [35]. The WSe_2 flake is excited by picosecond pulses generated by a tunable frequency-doubled optical parametric oscillator (OPO) synchronously pumped by a mode-locked Ti:Sa laser. The typical pulse and spectral width are 1.6 ps and 3 meV respectively; the repetition rate is 80 MHz. The laser power has been kept in the μW range in the linear absorption regime (see figure 5). The laser wavelength can be tuned between 500 and 740 nm. The detection spot diameter is $\approx$ 1 μm. For time-integrated experiments, the PL emission is dispersed in a spectrometer and detected with a Si-CCD camera. For time-resolved experiments, the PL signal is dispersed by an imaging spectrometer and detected by a synchro-scan Hamamatsu Streak Camera with an overall time resolution of 4 ps. The PL polarization P_c defined as $P_c = \frac{I_{\sigma+} - I_{\sigma-}}{I_{\sigma+} + I_{\sigma-}}$ is analyzed by a quarter-wave plate placed in front of a linear polarizer. Here $I_{\sigma+}(I_{\sigma-})$ denotes the intensity of the right (σ^+) and left (σ^-) circularly polarized emission.

Experimental Results.— For PL experiments the laser excitation energy is E_{Laser} = 1.893 eV, which is 140 meV above the neutral A-exciton emission energy and clearly below the B-exciton absorption as confirmed in reflectivity measurements (see figure 4). The time integrated PL emission at T=4K of the WSe_2 monolayer stems from the recombination of X^0, trions and localised excitons. These lines are very similar to the emission reported for this system in [20], where a bias was applied to the ML WSe_2. At this point it is unclear whether the trion emission stems from positively or negatively charged excitons. Considering the commonly observed residual n-type doping, the trion charge is assumed to be negative for the discussion below. Note that this assumption is not critical for ML WSe_2 as the spin-splitting of both the conduction band ($\approx$ 30 meV at $k = K_{\pm}$ [16, 19]) and valence band ($\approx$ 430 meV [2]) are substantial. The identification of the transitions is based on the polarization analysis shown in figures 1c and d. Under linearly polarized laser excitation, only the highest energy peak shows linear polarization in emission and is therefore ascribed to the X^0, as a coherent superposition of valley states is created [20]. This observation of exciton alignment is independent of the direction of the incident laser polarization, which confirms that the observed linear polarization is not due to macroscopic birefringence in the sample (see figure 9). The strong remaining coherence in figure 1d following non-resonant excitation hints at a direct optical generation of the neutral exciton X^0 for the laser energy used, energetically below the free carrier absorption and well below the B-exciton. Under circularly polarized excitation in figure 1c, the two highest energy transitions are strongly polarized, as expected for the X^0 and the trion. The clear separation by 30 meV of the trion (PL FWHM 15 meV) and neutral exciton (PL FWHM 10 meV) is a major advantage compared to current MoS_2 ML samples for the independent investigation of the valley dynamics. Energetically below the trion emission we record two emission peaks that we assign to localized exciton complexes and that are accordingly labelled L1 and L2.

In TRPL experiments we observe striking differences between the main transitions, as can be seen in figure 1e and figure 2. We first discuss the emission times, that can be compared in figure 2. The main X^0 emission time cannot be resolved by our experiment, it decays within 4ps as shown in figure 2, in a very similar way to ML MoS_2 [27]. As a result of the short PL emission time, the coherence time could be as short as a few ps and still result in a strong linear polarization degree of the time-integrated PL [20]. If the short X^0 emission time is limited by radiative recombination in this system with predicted

exciton binding energies of several hundred meV [25, 26] or by non-radiative processes, is still an open question. The weak PL emission at later times can be well fitted by a simple exponential decay with a characteristic time of 30 ps. The origin of this longer time may be attributed to exciton-phonon scattering, which scatters the exciton out of the light cone. The excitons have subsequently to reduce their momenta via scattering to return to the light cone to recombine radiatively [28, 36]. Another possible origin of the emission comes from neutral excitons localised at fluctuations of the Coulomb potential [37, 38]. Note that this type of weak localisation is qualitatively different from forming bound states such as the D^0X in GaAs, that might have parallels to the complexes L1 and L2.

The trion PL emission can be fitted by a bi-exponential decay. We observe no measurable risetime of the trion PL signal within our resolution. The initial trion decay is clearly longer than for the X^0 as can be seen already in figure 1e and we extract a decay time of about 18 ps, see figure 2. At longer times we extract an emission with a decay of 30ps, just as in the case of the X^0. In general the longer emission times allow for a more detailed polarization analysis in the case of the trion compared to the ultra-short X^0 emission. The trion emission time being longer than the X^0 emission time is a trend also observed in III-V [39] and II-VI [40] semiconductor quantum wells, where the longer trion emission time was ascribed to a lowering of the oscillator strength due to a stronger localisation.

For the peak labelled L1 we record a clear, mono-exponential decay. The majority of photons resulting from L1 recombination are emitted after the main X^0 and trion recombination, see figures 1e and 2. The decay time extracted here is 30ps. The considerably less intense transition L2 also decays mono-exponentially, albeit with a considerably longer characteristic time of 80s. In temperature dependent measurements, we find at T=100 K that the L2 emission is negligible compared to L1, X^0 and the trion lines (see figure 6). The emission times measured here for X^0, trion, L1 and L2 transitions remain essentially constant for the the laser excitation energies used (1.851, 1.893 and 1.968 eV), as documented in figure 7.

We now discuss the time evolution of the PL polarization that gives access to the valley dynamics. Due to the fast decay time of the main X^0 emission (limited by our temporal resolution), we cannot extract a meaningful polarization decay time. According to recent estimations [32, 33] neutral excitons from non-equivalent K valleys in TMDCs are coupled by the Coulomb exchange interaction. This could lead to a rapid decay of the optically

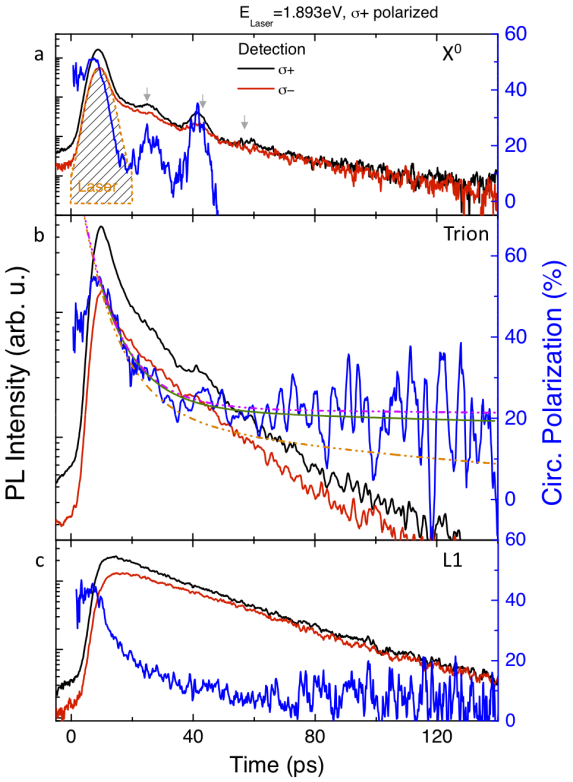

FIG. 3: **Time resolved photoluminescence.** T=4K. Laser polarization σ^+. (a) Left axis: X^0 PL emission (in log-scale) co-polarized (black) and cross-polarized (red) with respect to the excitation laser as a function of time. Right axis: circular polarization degree of the PL emission. As the PL intensity decays very quickly, we clearly observe a periodic signal of laser reflections, marked by arrows (b) same as (a), but for trion emission. The polarization well reproduced by a bi-exponential decay using an initial, fast decay time of 12 ps and a long decay time 1 ns (solid green line). Lower bounds (dotted orange line for 150ps) and upper bounds (dotted purple line for 3 ns) of the slow decay are shown. (c) same as (a), but for localized exciton emission L1.

initialized circular polarization, in close analogy to neutral exciton depolarization in GaAs quantum wells [31] and will contribute to the fast inter-valley relaxation decay observed in 1ML MoS_2 in pump-probe experiments [29, 30]. The coupling of a neutral exciton created with $\sigma+$ light in the K_+ valley to an exciton in the K_- valley is efficient as it does not rely on single carrier (electron or hole) spin flips, which are energetically forbidden.

The initial trion emission time is much longer than the one of the X^0 in figures 2 and 3b, it decays within a few tens of ps, well above the temporal resolution of our experiment. The longer trion emission time allows us to access the time evolution of the valley polarization:

We first observe an initial decay from 50% down to about 20% with a characteristic time of 12ps. Concerning the origin of this initial decay: The trion could be either generated directly following photon absorption (phonon assisted process), or by a localised electron capturing a free exciton. This second scenario is unlikely, as within the initial decay of 12ps the neutral exciton polarization would have already decayed to zero before capture, which is in contradiction with the strong, remaining valley polarization. For times $t >\approx 40\ ps$ we can infer a typical decay time of about 1ns for this substantial polarization, as indicated in figure 3b. Please note that a typical decay time of 150 ps gives an estimation that is clearly below the observed experimental polarization, whereas a decay time of 3 ns still gives a good fit (see dotted lines in figure 3b). The trion PL polarization dynamics show clear, experimental proof of the robustness of the optically initialised valley polarization. Measurements carried out at different laser excitation energies show similarly encouraging results (see figure 8). This is in contrast to ML MoS_2, which shows a strong decrease of the PL polarization when the laser excitation energy increases [23, 27]. This difference could be due to the fact that the Γ valence states are very close in energy to the K states (a few meV [41]) in MoS_2 whereas for WSe_2 the splitting energy is considerably larger.

The emission we labelled L1 shows a fast initial polarization decay with a characteristic time of about 13 ps before reaching a polarization plateau as in the trion case, albeit at a smaller value around 8%. In reference [20] in a gated WSe_2 ML structure a peak approximately at the energy of L1 was ascribed to a fine structure split trion state. Although the linewidth of the PL emission of the X^0, trion and L1 is considerably smaller than in MoS_2, we cannot extract any information at this stage concerning an eventual fine structure due to strong Coulomb exchange in this system [33], which might influence the observed polarization dynamics.

In conclusion, time resolved PL experiments in monolayer WSe_2 allow to access directly the valley dynamics by monitoring the charged exciton (trion) emission. We measure a valley polarization decay time longer than 1 ns. To verify valley stability beyond this time range pump-probe measurements are needed. Similar results can be expected for ML MoS_2, but are currently far more difficult to extract due to the broader (roughly 3.5×) linewidth at 4K and also 300K in exfoliated samples.

I. ACKNOWLEDGEMENTS

We acknowledge partial funding from ERC Starting Grant No. 306719 and Programme Investissements d'Avenir ANR-11-IDEX-0002-02, reference ANR-10-LABX-0037-NEXT. We thank I. Gerber and M.M. Glazov for stimulating discussions.

---

[1] A. K. Geim and I. V. Grigorieva, Nature **499**, 419 (2013).

[2] Z. Y. Zhu, Y. C. Cheng, and U. Schwingenschlögl, Phys. Rev. B **84**, 153402 (2011).

[3] K. F. Mak, C. Lee, J. Hone, J. Shan, and T. F. Heinz, Phys. Rev. Lett. **105**, 136805 (2010).

[4] A. Splendiani, L. Sun, Y. Zhang, T. Li, J. Kim, C.-Y. Chim, G. Galli, and F. Wang, Nano Letters **10**, 1271 (2010).

[5] W. Zhao, Z. Ghorannevis, L. Chu, M. Toh, C. Kloc, P.-H. Tan, and G. Eda, ACS Nano **7**, 791 (2013), http://pubs.acs.org/doi/pdf/10.1021/nn305275h, URL `http://pubs.acs.org/doi/abs/10.1021/nn305275h`.

[6] H. Fang, S. Chuang, T. C. Chang, K. Takei, T. Takahashi, and A. Javey, Nano Letters **12**, 3788 (2012), http://pubs.acs.org/doi/pdf/10.1021/nl301702r, URL `http://pubs.acs.org/doi/abs/10.1021/nl301702r`.

[7] W. Liu, J. Kang, D. Sarkar, Y. Khatami, D. Jena, and K. Banerjee, Nano Letters **13**, 1983 (2013), http://pubs.acs.org/doi/pdf/10.1021/nl304777e, URL `http://pubs.acs.org/doi/abs/10.1021/nl304777e`.

[8] H. Zeng, G.-B. Liu, J. Dai, Y. Yan, B. Zhu, R. He, L. Xie, S. Xu, X. Chen, W. Yao, et al., Scientific Reports **3**, 1608 (2013).

[9] J. S. Ross, P. Klement, A. M. Jones, N. J. Ghimire, J. Yan, D. G. Mandrus, T. Taniguchi, K. Watanabe, K. Kitamura, W. Yao, et al., ArXiv e-prints (2013), 1312.1435.

[10] R. S. Sundaram, M. Engel, A. Lombardo, R. Krupke, A. C. Ferrari, P. Avouris, and M. Steiner, Nano Letters **13**, 1416 (2013), http://pubs.acs.org/doi/pdf/10.1021/nl400516a, URL `http://pubs.acs.org/doi/abs/10.1021/nl400516a`.

[11] B. Radisavljevic, A. Radenovic, J. Brivio, V. Giacometti, and A. Kis, Nature. Nanotech. **6**, 147 (2011).

[12] N. Kumar, S. Najmaei, Q. Cui, F. Ceballos, P. M. Ajayan, J. Lou, and H. Zhao, Phys. Rev.

B **87**, 161403 (2013), URL http://link.aps.org/doi/10.1103/PhysRevB.87.161403.

[13] D. Xiao, G.-B. Liu, W. Feng, X. Xu, and W. Yao, Phys. Rev. Lett. **108**, 196802 (2012).

[14] A. Rycerz, J. Tworzydlo, and C. J. Beenakker, Nature. Phys. **3**, 172 (2007).

[15] Z. Zhu, A. Collaudin, B. Fauque, W. Kang, and K. Behnia, Nat. Phys. **8**, 89 (2012).

[16] G.-B. Liu, W.-Y. Shan, Y. Yao, W. Yao, and D. Xiao, Phys. Rev. B **88**, 085433 (2013), URL http://link.aps.org/doi/10.1103/PhysRevB.88.085433.

[17] T. Cao, G. Wang, W. Han, H. Ye, C. Zhu, J. Shi, Q. Niu, P. Tan, E. Wang, B. Liu, et al., Nature Communications **3**, 887 (2012).

[18] X. Li, F. Zhang, and Q. Niu, Phys. Rev. Lett. **110**, 066803 (2013), URL http://link.aps.org/doi/10.1103/PhysRevLett.110.066803.

[19] K. Kosmider, J. W. González, and J. Fernández-Rossier, Phys. Rev. B **88**, 245436 (2013), URL http://link.aps.org/doi/10.1103/PhysRevB.88.245436.

[20] A. M. Jones, H. Yu, N. J. Ghimire, S. Wu, G. Aivazian, J. S. Ross, B. Zhao, J. Yan, D. G. Mandrus, D. Xiao, et al., Nat. Nanotechnol. **8**, 634 (2013).

[21] K. F. Mak, K. He, J. Shan, and T. F. Heinz, Nat. Nanotechnol. **7**, 494 (2012).

[22] G. Sallen, L. Bouet, X. Marie, G. Wang, C. R. Zhu, W. P. Han, Y. Lu, P. H. Tan, T. Amand, B. L. Liu, et al., Phys. Rev. B **86**, 081301 (2012), URL http://link.aps.org/doi/10.1103/PhysRevB.86.081301.

[23] G. Kioseoglou, A. T. Hanbicki, M. Currie, A. L. Friedman, D. Gunlycke, and B. T. Jonker, Applied Physics Letters **101**, 221907 (pages 4) (2012), URL http://link.aip.org/link/?APL/101/221907/1.

[24] S. Wu, C. Huang, G. Aivazian, J. S. Ross, D. H. Cobden, and X. Xu, ACS Nano **7**, 2768 (2013), http://pubs.acs.org/doi/pdf/10.1021/nn4002038, URL http://pubs.acs.org/doi/abs/10.1021/nn4002038.

[25] D. Y. Qiu, F. H. da Jornada, and S. G. Louie, Phys. Rev. Lett. **111**, 216805 (2013), URL http://link.aps.org/doi/10.1103/PhysRevLett.111.216805.

[26] A. Ramasubramaniam, Phys. Rev. B **86**, 115409 (2012), URL http://link.aps.org/doi/10.1103/PhysRevB.86.115409.

[27] D. Lagarde, L. Bouet, X. Marie, C. R. Zhu, B. L. Liu, T. Amand, P. H. Tan, and B. Urbaszek, Phys. Rev. Lett. **112**, 047401 (2014), URL http://link.aps.org/doi/10.1103/PhysRevLett.112.047401.

[28] T. Korn, S. Heydrich, M. Hirmer, J. Schmutzler, and C. Schüller, Applied Physics Letters **99**, 102109 (2011).

[29] C. Mai, A. Barrette, Y. Yu, Y. G. Semenov, K. W. Kim, L. Cao, and K. Gundogdu, Nano Letters **14**, 202 (2014), http://pubs.acs.org/doi/pdf/10.1021/nl403742j, URL http://pubs.acs.org/doi/abs/10.1021/nl403742j.

[30] Q. Wang, S. Ge, X. Li, J. Qiu, Y. Ji, J. Feng, and D. Sun, ACS Nano **7**, 11087 (2013), http://pubs.acs.org/doi/pdf/10.1021/nn405419h, URL http://pubs.acs.org/doi/abs/10.1021/nn405419h.

[31] M. Z. Maialle, E. A. de Andrada e Silva, and L. J. Sham, Phys. Rev. B **47**, 15776 (1993), URL http://link.aps.org/doi/10.1103/PhysRevB.47.15776.

[32] T. Yu and M. W. Wu, ArXiv e-prints (2014), 1401.0047.

[33] H. Yu, G. Liu, P. Gong, X. Xu, and W. Yao, ArXiv e-prints (2014), 1401.0667.

[34] K. S. Novoselov, D. Jiang, F. Schedin, T. J. Booth, V. V. Khotkevich, S. V. Morozov, and A. K. Geim, Proc. Natl Acad. Sci. USA **102**, 10451 (2005).

[35] G. Sallen, B. Urbaszek, M. M. Glazov, E. L. Ivchenko, T. Kuroda, T. Mano, S. Kunz, M. Abbarchi, K. Sakoda, D. Lagarde, et al., Phys. Rev. Lett. **107**, 166604 (2011).

[36] D. Sanvitto, R. A. Hogg, A. J. Shields, D. M. Whittaker, M. Y. Simmons, D. A. Ritchie, and M. Pepper, Phys. Rev. B **62**, R13294 (2000), URL http://link.aps.org/doi/10.1103/PhysRevB.62.R13294.

[37] B. Deveaud, F. Clérot, N. Roy, K. Satzke, B. Sermage, and D. S. Katzer, Phys. Rev. Lett. **67**, 2355 (1991), URL http://link.aps.org/doi/10.1103/PhysRevLett.67.2355.

[38] T. Amand, J. Barrau, X. Marie, N. Lauret, B. Dareys, M. Brousseau, and F. Laruelle, Phys. Rev. B **47**, 7155 (1993), URL http://link.aps.org/doi/10.1103/PhysRevB.47.7155.

[39] G. Finkelstein, V. Umansky, I. Bar-Joseph, V. Ciulin, S. Haacke, J.-D. Ganière, and B. Deveaud, Phys. Rev. B **58**, 12637 (1998), URL http://link.aps.org/doi/10.1103/PhysRevB.58.12637.

[40] E. Vanelle, M. Paillard, X. Marie, T. Amand, P. Gilliot, D. Brinkmann, R. Lévy, J. Cibert, and S. Tatarenko, Phys. Rev. B **62**, 2696 (2000), URL http://link.aps.org/doi/10.1103/PhysRevB.62.2696.

[41] A. Kormányos, V. Zólyomi, N. D. Drummond, P. Rakyta, G. Burkard, and V. I. Fal'ko, Phys. Rev. B **88**, 045416 (2013), URL http://link.aps.org/doi/10.1103/PhysRevB.88.045416.

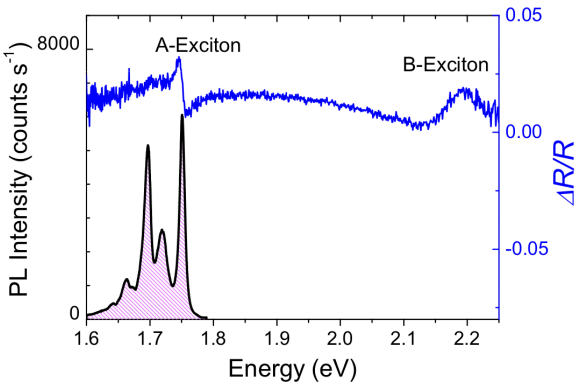

FIG. 4: T=4K. The position of the neutral A-exciton emission (blue curve) is confirmed in reflectivity measurements (blue curve) compared to the PL emission of the A-exciton (black curve). We measure an energy difference between A- and B- exciton of 410 ± 15 meV, in good agreement with theory [2] and values extracted from hot PL emission [8].

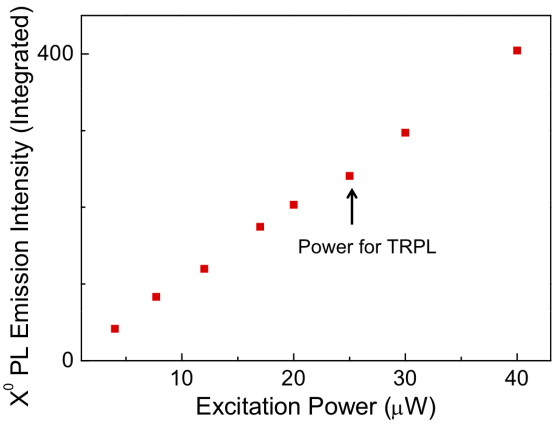

FIG. 5: T=4K. The time resolved measurements were carried out at low power well within the linear absorption regime. The laser power was kept low in all experiments (i) to avoid sample damage, a problem studied in detail in Raman experiments [42] (ii) to avoid secondary emission from high signal levels of the phosphorus screen of the streak camera.

[42] H. Li, G. Lu, Y. Wang, Z. Yin, C. Cong, Q. He, L. Wang, F. Ding, T. Yu, and H. Zhang, Small **9**, 1974 (2013), ISSN 1613-6829, URL `http://dx.doi.org/10.1002/smll.201202919`.

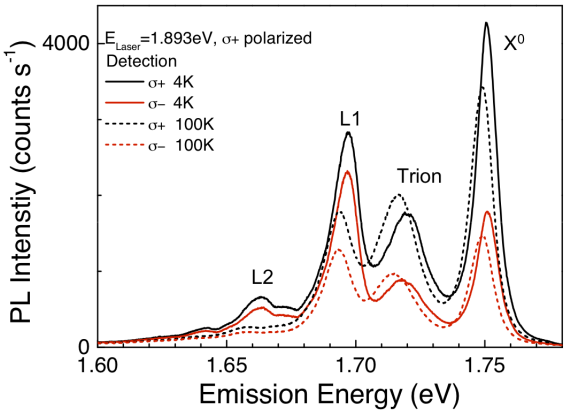

FIG. 6: The PL intensity of the peak L2 is strongly reduced when comparing the spectra at 4K and 100K, confirming the localised nature of the emission.

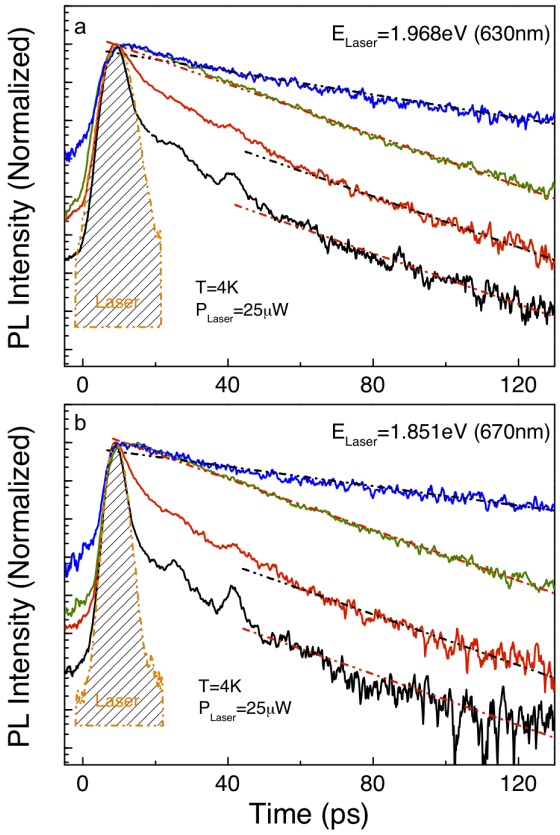

FIG. 7: **Emission time for different excitation laser energies.** The PL emission is shown for two additional laser excitation energies E_{Laser} as compared to the main text. The color code is the same as in the main text: X^0 - black, Trion - red, L1 - green and L2 - blue. The decay times (fits indicated by dotted lines) are the same as for $E_{Laser} = 1.893$ eV used in the main text for X^0, Trion and L1. The L2 decay time in (a) is 65 ps and in (b) 78 ps.

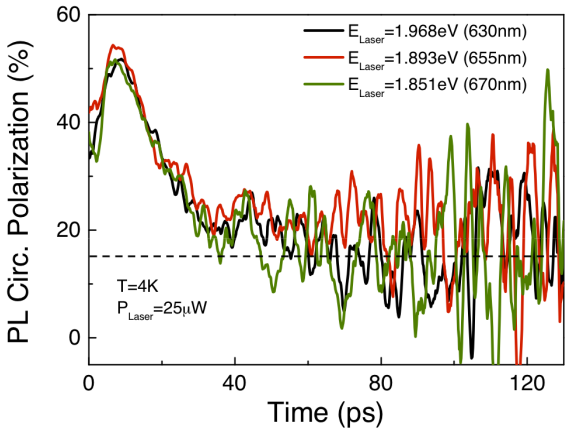

FIG. 8: **Valley dynamics monitored through trion emission for different excitation laser energies.** The time evolution of the PL polarization i.e. the valley dynamics is plotted for the trion using three different excitation laser energies. In all three cases the dynamics is very similar, with a long lasting, stable polarization after an initial, fast decay. The dashed line is a guide to the eye.

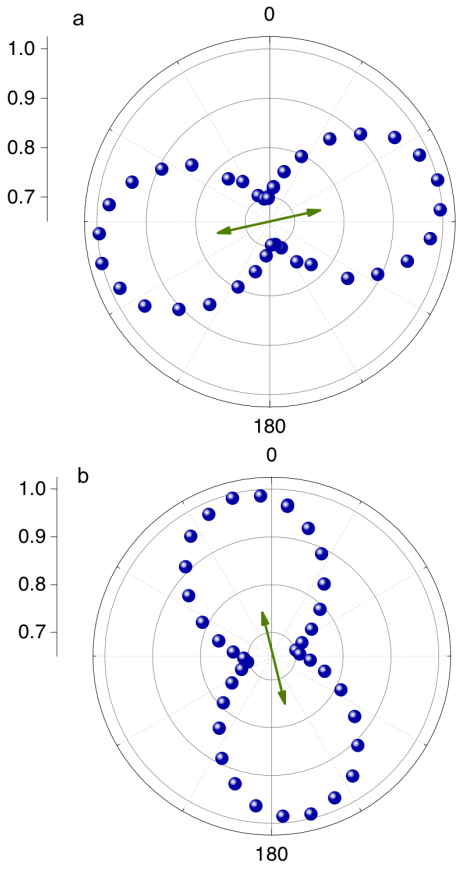

FIG. 9: **Valley coherence of neutral exciton X^0.** T=4K. The excitation laser polarization is linear. Here the time integrated PL emission intensity of the X^0 is plotted as a function of the angle of the linear polariser in the detection path for different linear polarization planes of the excitation laser (a) and (b). The X^0 polarization plane follows the excitation laser and is not linked to a specific lattice axis or symmetry, which confirms the generation of neutral exciton valley coherence [20]